Color Image Watermarking Using Selective MSB-LSB Embedding And 2D Otsu Thresholding

Thien Huynh-The, Sungyoung Lee
Department of Computer Science and Engineering
Kyung Hee University, Gyeonggi-do, 446-701, Korea
Email: {thienht,sylee}@oslab.khu.ac.kr

***Abstract*—This paper proposes a novel digital image watermarking method, namely SMLE, that allows to intelligently embed a gray-scale watermark image into a color host image in the wavelet domain. By decomposing a gray-scale image to binary images in digits ordering from Least Significant Bit (LSB) to Most Significant Bit (MSB), binary bits are efficiently embedded to optimal wavelet coefficient blocks using a quantization technique which encodes wavelet coefficient differences to either of two pre-identified thresholds for corresponding 0-bits or 1-bits. To boost visual quality, an embedding rule is improved by equal spreading coefficient adjustment on two middle-frequency sub-bands instead of only one as existing approaches. Additionally, 2D Otsu algorithm, more proficient than 1D Otsu algorithm for binary classification under attacking scenarios, is modified to flexibly calculate an optimal threshold for high-rate watermark extraction. According to experimental results, our proposed SMLE watermarking model produces remarkable imperceptibility as well as high robustness against common digital image transformations and mostly does better than other existing methods at same payload rate.**

***Keywords*—Color image watermarking, selective MSB-LSB embedding, wavelet coefficient quantization, 2D Otsu thresholding.**

I. Introduction

Fostered by the rapid growth of mobile devices and the Internet, the creation and sharing of digital images are ubiquitously captured to reflect daily personal and social life. Some critical challenges relating to transmission, storage, and especially usage are highly noticeable in which the copyright protection plays a crucial role. If image sharing is not protected for free access, download and re-usage by others illegally, personal images might become subjects to commercial or other purposes by third parties without an owner consent. To prevent such kind of problems, efficient and robust digital watermarking techniques are urgently required for copyright protection and authentication [1], [2].

Watermarking techniques can be categorized based on: i) processing domain such as spatial domain and frequency domain, and ii) extraction requirement such as blind, semi-blind, and non-blind watermarking schemes. Due to natural limitations of spatial domain based techniques, i.e., high perceptibility of a host image and fragility of a watermark under image processing operations, most image watermarking techniques spread hidden information on the frequency domain [3]–[6]. To be against geometric distortions, Niu et al. [3] combined Nonsubsampled Contourlet Transform (NSCT) and Support Vector Regression (SVR), however, the quality of embedded images was quite worse than others in the field. A wavelet quantization technique for blind watermarking was developed by Run et al. [4], but it was defeated by some common attacks such as rotation and lossy JPEG compression due to constant thresholding used for watermark extraction. Nezhadarya et al. [5] proposed an angle quantization technique, called Gradient Direction Watermarking (QDWM) in which binary bits were encoded into wavelet directional gradients using Absolute Angle Quantization Index Modulation (AAQIM). Extreme Learning Machine (ELM) [6], a fast learning algorithm commonly used for Single Hidden Layer Feedforward Neural Networks (SLFNs), was performed in the wavelet domain to reach a pleasant tradeoff between imperceptibility and robustness. Since the above approaches are principally introduced to embed binary information, e.g., images and bit sequences are encoded into gray-scale or color images, they therefore offered poor payload capacity, usually measured by an embedding rate factor. Recently, Saboori et al. [7] combined Principle Component Analysis (PCA) and a histogram matching technique on the luminance component of YUV color space to embed a gray-scale watermark into a color host image. Although the method delivered high imperceptibility of watermarked images, it was weakly against common attacks such as digital filtering, rotation, and additional noise.

In this work, we propose a blind digital image watermarking model, namely Selective MSB-LSB Embedding (SMLE), for color host images. Concretely, a gray-scale watermark image is decomposed to component binary images following LSB-MSB digits ordering and then encoded into a host image onto middle-frequency sub-bands in the wavelet domain. Compared to the existing work [8], we further improve an embedding rule by equally spreading quantization adjustment on two sub-bands simultaneously to minimize the total coefficient alternation. This leads to an increment of the embedded image quality as well. In the extraction stage, an adaptive threshold for binary bit classification is calculated by 2D Otsu algorithm which is more efficient than 1D Otsu for hash conditions. We benchmark SMLE with several common color host images and gray-scale watermarks under various embedding strength levels. Based on experimental evaluation, our proposed SMLE achieves a high performance in terms of imperceptibility and robustness, and so far outperforms existing approaches at same payload capacity.

The remaining of this paper is organized as follows. The second section describes our proposed watermarking model. Experimental results are reported and discussed in the third section. Finally, conclusions are outlined in the fourth section.

978-1-5090-1897-0/16/$31.00

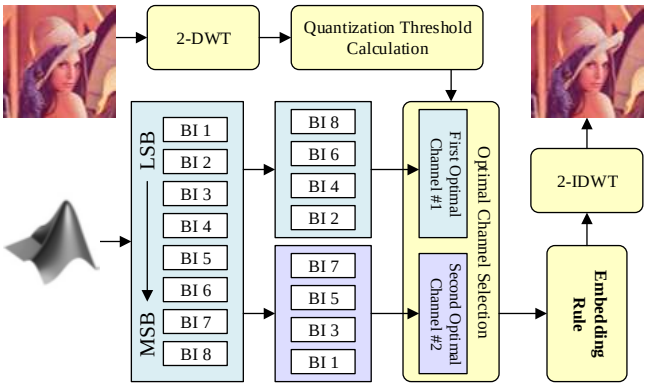

Fig. 1. The workflow of embedding process. The gray-scale watermark is decomposed from a 8-bit image to 8 binary images (BIs) representing digits ordering from LSB to MSB.

II. The Proposed Methodology

This section presents SMLE, an efficient image watermarking method where a gray-scale watermark is embedded to a color image. Both watermark embedment and extraction are processed in the wavelet domain, concretely, a 64×64 image is encoded into coefficients of the horizontal LH (low-high) and vertical HL (high-low) sub-bands of a 512×512 host image using Discrete Wavelet Transform (DWT).

A. Watermark Embedding Process

At first, a gray-scale watermark image $\boldsymbol{W}$ is decomposed to eight binary images $\boldsymbol{w}_{b1:b8}$ which represents digits ordering from LSB to MSB as shown in Fig. 1. These binary bits are then embedded to a host color image $\boldsymbol{I}$ by a quantization technique in which HL-LH coefficient differences $\Delta_{i,k} = \left|HL_i^k - LH_i^k\right|$ of i^{th} wavelet block in k^{th} color channel are quantized to predefined thresholds δ_0 and δ_1 for 0-bits and 1-bits respectively by altering wavelet coefficients. Following [8], wavelet blocks are sorted in the ascending order of difference, denoted $\Delta_{i,k}^S$, to encode 0-bits for smallest difference blocks and 1-bits for greatest difference blocks. Two optimal color channels are chosen for binary embedding to minimize the differences between $\Delta_{i,k}^S$ and δ_0 for binary bit $w_i = 0$ and δ_1 for $w_i = 1$. In particular, the watermark bits of four binary images $\boldsymbol{w}_{k^{\#1}} = \{\boldsymbol{w}_{b2}, \boldsymbol{w}_{b4}, \boldsymbol{w}_{b6}, \boldsymbol{w}_{b8}\}$ are encoded to the first optimal channel $k^{\#1}$ and the watermark bits of remaining images $\boldsymbol{w}_{k^{\#2}} = \{\boldsymbol{w}_{b1}, \boldsymbol{w}_{b3}, \boldsymbol{w}_{b5}, \boldsymbol{w}_{b7}\}$ are then encoded to the second optimal channel $k^{\#2}$. The channel selection is defined as follows

$$k^{\#1} = \begin{cases} \arg\min\limits_k \left(\left|\Delta_{i,k}^S - \delta_0\right|\right) & \forall w_i \in \boldsymbol{w}_{k^{\#1}} = 0 \\ \arg\min\limits_k \left(\left|\Delta_{i,k}^S - \delta_1\right|\right) & \forall w_i \in \boldsymbol{w}_{k^{\#1}} = 1 \end{cases}$$
$$k^{\#2} = \begin{cases} \arg\min\limits_k \left(\left|\Delta_{i,-k^{\#1}}^S - \delta_0\right|\right) & \forall \boldsymbol{w}_i \in w_{k^{\#2}} = 0 \\ \arg\min\limits_k \left(\left|\Delta_{i,-k^{\#1}}^S - \delta_1\right|\right) & \forall \boldsymbol{w}_i \in w_{k^{\#2}} = 1 \end{cases} \tag{1}$$

The notation $-k^{\#1}$ indicates remaining color channels except $k^{\#1}$. Two quantization thresholds are calculated following (8) where N_0 and N_1 are the number of 0-bits and 1-bits of $\boldsymbol{w}_{b1:b8}$; λ is the robustness factor representing embedding strength of a watermark on a host image. A large value of λ deeply embeds a watermark into a host image, i.e., a watermark is more robust under several digital image transformations while its imperceptibility on a host image is worse and worse. Therefore, λ should be flexibly selected for a reasonable balance between watermark robustness and image imperceptibility. For watermark embedment execution, an improved rule is generally applied as follows (placing k^* by $k^{\#1}$ and $k^{\#2}$ as two optimal channels corresponding to binary watermarks in $\boldsymbol{w}_{k^{\#1}}$ and $\boldsymbol{w}_{k^{\#2}}$ respectively)

For 0-bits encoding

If $\Delta_{i,k^*}^S > \delta_0$

$$\begin{aligned} LH_i^{k^*} \geq HL_i^{k^*} \rightarrow \begin{cases} LH_i^{k^*} = LH_i^{k^*} - \nabla_i^0/2 \\ HL_i^{k^*} = HL_i^{k^*} + \nabla_i^0/2 \end{cases} \\ LH_i^{k^*} < HL_i^{k^*} \rightarrow \begin{cases} LH_i^{k^*} = LH_i^{k^*} + \nabla_i^0/2 \\ HL_i^{k^*} = HL_i^{k^*} - \nabla_i^0/2 \end{cases} \end{aligned} \tag{2}$$

If $\Delta_{i,k^*}^S \leq \delta_0$

$$\begin{aligned} LH_i^{k^*} &= LH_i^{k^*} \\ HL_i^{k^*} &= HL_i^{k^*} \end{aligned} \tag{3}$$

For 1-bits encoding

If $\Delta_{i,k^*}^S < \delta_1$

$$\begin{aligned} LH_i^{k^*} \geq HL_i^{k^*} \rightarrow \begin{cases} LH_i^{k^*} = LH_i^{k^*} + \nabla_i^1/2 \\ HL_i^{k^*} = HL_i^{k^*} - \nabla_i^1/2 \end{cases} \\ LH_i^{k^*} < HL_i^{k^*} \rightarrow \begin{cases} LH_i^{k^*} = LH_i^{k^*} - \nabla_i^1/2 \\ HL_i^{k^*} = HL_i^{k^*} + \nabla_i^1/2 \end{cases} \end{aligned} \tag{4}$$

If $\Delta_{i,k^*}^S \geq \delta_1$

$$\begin{aligned} LH_i^{k^*} &= LH_i^{k^*} \\ HL_i^{k^*} &= HL_i^{k^*} \end{aligned} \tag{5}$$

where $\nabla_i^0 = \Delta_{i,k^*}^S - \delta_0$ and $\nabla_i^1 = \delta_1 - \Delta_{i,k^*}^S$ represent the modification of original coefficients required for encoding 0-bits and 1-bits, respectively. Compared to [8] where the modification is employed on either LH or HL by ∇_i^0 or ∇_i^1, we split them equally for two sub-bands to preserve the visual quality of watermarked images.

When the embedding process is completed, the modified coefficient differences are either less than δ_0 or greater than δ_1. Each color channel is recovered by Inverse Discrete Wavelet Transform (IDWT). Moreover, an associated key containing the information of channel blocks is generated and maintained for original watermark recovery during the extraction process.

B. Watermark Extraction Process

The first step in extraction process is to calculate the DWT coefficient differences of encoded blocks with a key, created in the embedding stage to contain the channel and block information. With a classification threshold, denoted δ_Δ where $\delta_0 < \delta_\Delta < \delta_1$, watermark bits are basically recovered by a comparison rule

$$w_i = \begin{cases} 1 & \forall \Delta_{i,k^*} \geq \delta_\Delta \\ 0 & otherwise \end{cases} \tag{6}$$

It is important to note that δ_Δ must be determined with the unknown quantization thresholds of δ_0 and δ_1. Therefore, an adaptive two-dimensional (2D) Otsu threshold [9], regularly used for image segmentation, is calculated to classify

$$(\delta_0 = \upsilon, \delta_1 = \upsilon + \lambda) = \arg\min_{\upsilon} \left(\sum_{m=i|\Delta_i^S > \upsilon}^{N_0} \left(\Delta_m^S - \upsilon\right) + \sum_{n=N_0+1}^{K|\Delta_K^S = \upsilon+\lambda} \left(\upsilon + \lambda - \Delta_n^S\right) \right) \quad (8)$$

Fig. 2. Test images used for evaluation. Top row: Lena, Mandrill, Peppers, and Barbara as host images; middle row: Matlab, Burger King, Firefox, and Starbucks as watermarks; and bottom row: Eight binary component images are decomposed from the Matlab sample.

DWT blocks which present 0-bits and 1-bits embedment. By maximizing the trace of between-class variance matrix $\boldsymbol{S_b}$, a threshold vector $(s = \delta_\Delta, t)$ is selected:

$$(s,t) = \begin{array}{c} \arg\max \\ 0 \le s \le L \\ 0 \le t \le L \end{array} \left(Tr\left(S_b\right)\right) \quad (7)$$

where $L = \max(\Delta_{i,k^*})$ and the trace of discrete matrix is expressed as follows (more details in Appendix):

$$Tr\left(S_b\right) = \frac{\left(\mu_{Ti}\omega_0 - \mu_i\right)^2 + \left(\mu_{Tj}\omega_0 - \mu_j\right)^2}{\omega_0\left(1-\omega_0\right)} \quad (8)$$

In the paper, a fast recursive algorithm of 2D Otsu [10] is employed to obtain the optimal threshold s. Compared to 1D Otsu [11], 2D Otsu algorithm handles as well to the noise segmentation challenge thanks to its contents-independent characteristics. A gray-scale watermark image is finally reconstructed following digits ordering from eight recovered binary images.

III. SIMULATION RESULTS AND DISCUSSION

In this section, we evaluate the perceptibility of embedded images and the robustness of watermarks under various popular image transformations. Four 512×512 color images served as host images and four 64×64 gray-scale images used as watermark images are shown in Fig. 2. Color Peak Signal-To-Noise (CPSNR) and Structural Similarity Index (SSIM) are used to measure the quality of watermarked images, i.e., the perceptibility of a watermark in host images. The extraction performance is quantitatively benchmarked by Normalized Cross-Correlation coefficient (NCC) which approaches to unity for high robustness.

A. Watermark Perceptibility

This section analyzes watermark perceptibility after the embedment process by evaluating the visual quality of watermarked images. The impact of robustness factor λ utilized to calculate quantization thresholds δ_0 and δ_1 is further considered. Table I reports the average CPSNR and SSIM of four samples on various values of λ with different watermarks. Obviously, the lower the λ is, the higher the CPSNR and SSIM achieve due to the less wavelet coefficient modification of the improved embedding rule. However a watermark will be more fragile under outside attacks because a small distance between δ_0 and δ_1 can not guarantee a high-quality extraction. Therefore, λ should be selected for a pleasant tradeoff between watermark robustness and host image imperceptibility.

TABLE I. AVERAGE PSNR AND SSIM OF EMBEDDED HOST IMAGES

λ	CPSNR (dB)			
	Matlab	Burger King	Firefox	Starbucks
20	48.27±3.66	49.66±2.77	50.25±1.28	49.54±2.56
25	45.24±3.33	46.85±3.34	47.55±2.08	46.83±3.28
30	42.77±3.06	44.51±3.46	45.35±2.64	44.52±3.47
35	40.74±2.78	42.47±3.36	43.53±3.03	42.48±3.37
40	39.06±2.51	40.43±3.13	41.89±3.17	40.70±3.15
45	37.62±2.29	38.89±3.90	40.37±3.14	39.15±2.91
50	36.34±2.15	37.54±2.69	39.00±3.01	37.81±2.69
λ	SSIM			
	Matlab	Burger King	Firefox	Starbucks
20	0.999±0.001	0.999±0.001	0.999±0.001	0.999±0.001
25	0.998±0.001	0.999±0.001	0.999±0.001	0.999±0.001
30	0.997±0.002	0.998±0.001	0.999±0.001	0.998±0.001
35	0.995±0.003	0.997±0.002	0.998±0.001	0.997±0.002
40	0.993±0.005	0.995±0.003	0.997±0.001	0.995±0.003
45	0.991±0.007	0.994±0.004	0.995±0.003	0.994±0.004
50	0.988±0.008	0.992±0.006	0.994±0.004	0.992±0.006

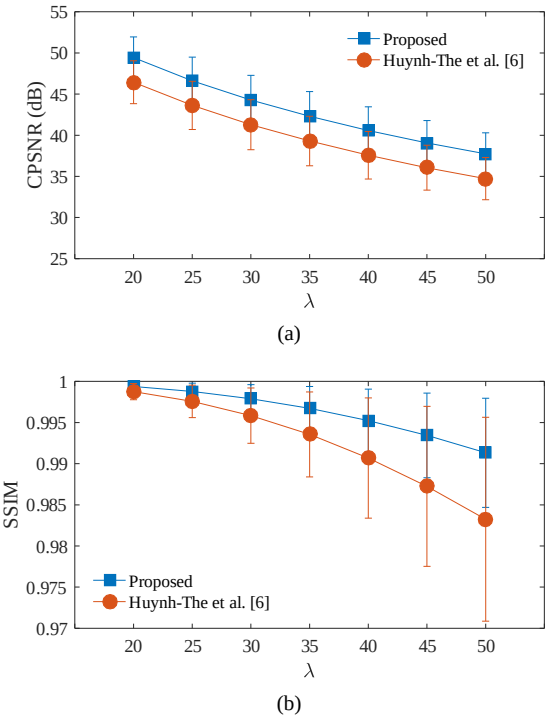

Fig. 3. Watermark perceptibility comparison between the proposed embedding rule and Huynh-The et al. [8] scheme: (a) CPSNR, (b) SSIM.

Fig. 4. Popular transformations on embedded image of Lena (left to right of two first rows): Non-Attack, Median Filtering 5×5, Average Filtering 5×5, Motion Blurring 5 pixels, Down-Scaling 128×128, Rotation 0.5^0, Cropping 128×128, Gaussian Noise $\left(\mu = 0, \sigma^2 = 0.0025\right)$, Salt & Pepper Noise $(density = 5\%)$, and Lossy JPEG Compression $(Quality = 70\%)$. The bottom row shows the corresponding extracted watermarks.

Compared to the previous rule [8], the embedding rule in this paper is significantly improved to boost the quality of watermarked images. With the quantitative results plotted in Fig. 3, our improved rule is entirely better, approximately 3dB of CPSNR and 0.004 of SSIM.

B. Watermark Robustness

This section explores the ability of our proposed method in recovering hidden information against digital image transformations like attack operations. For the latter, popular transformations in the field are median filtering, average filtering, linear motion blurring, size scaling, rotation, cropping, additional noise (Gaussian and Salt & Pepper), and lossy JPEG compression. Fig. 4 illustrates the transformations and their corresponding extracted watermarks with Lena and Matlab samples. The NCC values of recovered watermarks corresponding to aforementioned attacks are reported in Table II with various values of λ. It is noted that the results are delivered as the average of four host images associated with four watermarks. The robustness is typically improved regarding the increment of λ. However, our model reports quite poor results with rotation and scaling due to following reasons: i) DWT decomposes an image in the horizontal and vertical dimensions while rotation operates in the diagonal, ii) scaling operation makes the loss of detail information through bicubic interpolation. The robustness is further investigated with median filtering, average filtering, motion blurring, and lossy JPEG compression under various intensities as plotted in Fig. 5. As a result, the stronger the attack damages are, the lower accuracy the watermark is generally recovered.

To prove the efficiency of 2D Otsu compared to 1D Otsu for watermark extraction, we evaluate robustness with two different thresholding algorithms. Table III presents NCC results of recovered watermarks in which 2D Otsu extracts more precisely for median filtering, average filtering, and motion blurring, especially in high levels of attacking. Although 2D Otsu looks more reliable than 1D Otsu in the task of calculating a high-rate threshold for watermark extraction, it requires high computational resource and performs unexpectedly in lossy JPEG compression.

In the last experiment, we compare SMLE with Saboori's approach in terms of watermark robustness as shown in Table IV. Saboori et al. [7] embedded a gray-scale watermark image into a color host image following two color mode strategies, e.g., the blue channel of RGB and the luminance channel of YUV. Although our proposed method performs worse in term of image imperceptibility as 39.48 dB vs 40.88 dB and 40.26 dB of RGB-B and YUV-Y respectively, it remarkably outperforms Saboori's approach in the most of digital image transformations, except the lossy JPEG compression. It should be noted that SMLE results in Table IV are reported as the average of Lena sample with various watermarks.

TABLE III. NCC COMPARISON BETWEEN 2D OTSU AND 1D OTSU ALGORITHM FOR WATERMARK EXTRACTION USING $\lambda = 40$

Median Filtering			**Average Filtering**		
Size	1D Otsu	2D Otsu	Size	1D Otsu	2D Otsu
3×3	0.900 ± 0.066	0.895 ± 0.080	3×3	0.900 ± 0.079	0.894 ± 0.088
5×5	0.706 ± 0.107	0.720 ± 0.114	5×5	0.668 ± 0.108	0.666 ± 0.108
7×7	0.621 ± 0.120	0.639 ± 0.128	7×7	0.559 ± 0.117	0.574 ± 0.126
9×9	0.579 ± 0.119	0.597 ± 0.130	9×9	0.497 ± 0.117	0.507 ± 0.122
11×11	0.535 ± 0.112	0.559 ± 0.122	11×11	0.443 ± 0.111	0.452 ± 0.117
Motion Blurring			**JPEG Compression**		
No.Pixels	1D Otsu	2D Otsu	QF (%)	1D Otsu	2D Otsu
3	0.923 ± 0.087	0.914 ± 0.083	10	0.693 ± 0.049	0.660 ± 0.065
5	0.815 ± 0.097	0.806 ± 0.102	30	0.828 ± 0.069	0.824 ± 0.058
7	0.713 ± 0.091	0.723 ± 0.095	50	0.852 ± 0.073	0.872 ± 0.044
9	0.637 ± 0.065	0.640 ± 0.063	70	0.865 ± 0.081	0.875 ± 0.069
11	0.578 ± 0.064	0.579 ± 0.065	90	0.902 ± 0.080	0.914 ± 0.056

TABLE IV. METHOD COMPARISON IN THE TERM OF ROBUSTNESS FOR LENA SAMPLE

Image Transformation	Saboori et al. [7] RGB-B	Saboori et al. [7] YUV-Y	SMLE ($\lambda = 35$)
MedFilt 3×3	0.8510	0.8876	**0.9574**
AverFilt 3×3	0.8454	0.8512	**0.9575**
GaussFilt 3×3	0.9717	0.9788	**0.9999**
Rotate 0.25^0	0.6234	0.6566	**0.8519**
Gaussian Noise	0.8101	0.8838	**0.8902**
Salt & Pepper Noise	0.9126	0.9488	**0.9943**
JPEG 20%	0.5543	0.6778	**0.7235**
JPEG 50%	0.6356	**0.9060**	0.8740
JPEG 70%	0.7456	**0.9820**	0.8854
JPEG 90%	0.9188	**0.9836**	0.8944

IV. CONCLUSION

A novel digital color image watermarking method, called Selective MSB-LSB Embedding (SMLE), has been proposed in this work. By decomposing a gray-scale image to binary images in which the digits order from LSB to MSB, a gray-scale watermark is encoded into a color host image using a quantization technique in the wavelet domain. Besides a color channel selection, the quality of watermarked images is significantly improved with an optimal embedding rule which minimizes the total wavelet coefficient modification. In addition, 2D Otsu algorithm is more efficient to extract watermark under various digital image transformations compared to 1D Otsu algorithm. The experimental results prove that our proposed SMLE watermarking model achieves a high performance in imperceptibility of embedded host images and robustness of extracted watermarks. The proposed method generally outperforms other similar watermarking approaches, except the test of lossy JPEG compression. In the future, we continuously validate the method on various large datasets and improve the extraction accuracy for lossy JPEG compression.

TABLE II. NCC OF EXTRACTED WATERMARKS UNDER DIFFERENT IMAGE TRANSFORMATIONS

Image Transformation	λ 20	25	30	35	40	45	50
Non-Attack	0.988 ± 0.017	0.991 ± 0.017	0.993 ± 0.015	0.994 ± 0.013	0.995 ± 0.012	0.999 ± 0.003	0.997 ± 0.010
MedFilt 5×5	0.697 ± 0.092	0.695 ± 0.098	0.707 ± 0.104	0.715 ± 0.110	0.720 ± 0.114	0.702 ± 0.104	0.705 ± 0.108
AverFilt 5×5	0.658 ± 0.100	0.658 ± 0.101	0.669 ± 0.109	0.669 ± 0.111	0.666 ± 0.108	0.666 ± 0.109	0.661 ± 0.109
Blurring 5 pixels	0.765 ± 0.090	0.788 ± 0.082	0.797 ± 0.089	0.804 ± 0.097	0.806 ± 0.102	0.810 ± 0.106	0.818 ± 0.109
Down-Scaling 128×128	0.532 ± 0.103	0.538 ± 0.104	0.553 ± 0.116	0.562 ± 0.125	0.565 ± 0.128	0.567 ± 0.132	0.571 ± 0.137
Rotation 0.5^0	0.597 ± 0.089	0.597 ± 0.087	0.610 ± 0.086	0.614 ± 0.089	0.615 ± 0.094	0.613 ± 0.095	0.619 ± 0.097
Cropping 128×128	0.892 ± 0.042	0.894 ± 0.040	0.895 ± 0.038	0.895 ± 0.037	0.896 ± 0.036	0.902 ± 0.041	0.902 ± 0.040
Gaussian Noise	0.682 ± 0.169	0.694 ± 0.155	0.724 ± 0.125	0.752 ± 0.099	0.790 ± 0.075	0.818 ± 0.054	0.838 ± 0.048
Salt & Pepper Noise	0.505 ± 0.182	0.650 ± 0.127	0.679 ± 0.130	0.718 ± 0.049	0.693 ± 0.075	0.652 ± 0.156	0.635 ± 0.172
JPEG 70%	0.847 ± 0.086	0.853 ± 0.075	0.862 ± 0.065	0.867 ± 0.061	0.857 ± 0.076	0.852 ± 0.075	0.849 ± 0.075

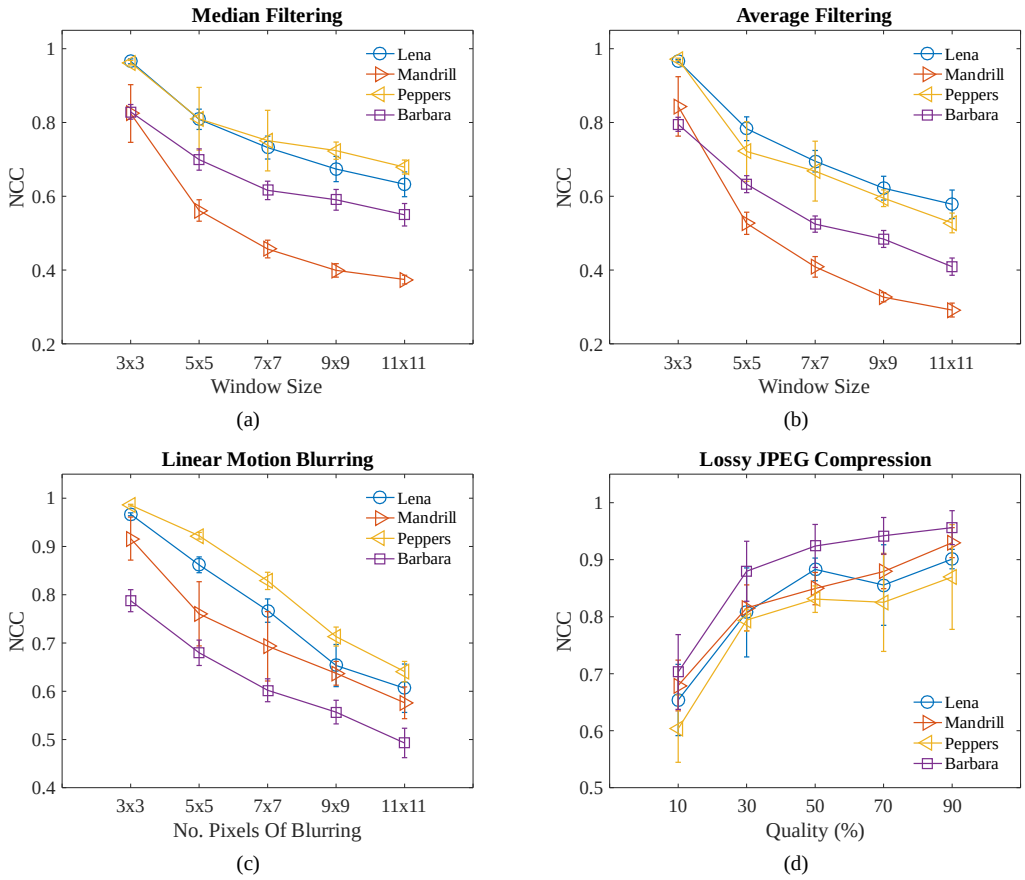

Fig. 5. Average watermark extraction accuracy measured by NCC using $\lambda = 40$ with four watermarks under various image transformations: (a) Median Filtering, (b) Average Filtering, (c) Motion Blurring, and (d) Lossy JPEG Compression.

APPENDIX
2D OTSU ALGORITHM

Suppose a gray-scale image with the size of $M \times N$ is presented by a gray level intensity $f(x, y)$ and its corresponding local average $g(x, y)$, ranging from 0 to $L-1$, where L is the number of gray levels. Let q_{ij} is the total number of occurrence (or frequency) of the pair (i, j) which is formed by $f(x, y) = i$ and $g(x, y) = j$. The joint probability mass function in 2-dimensional histogram is defined:

$$p_{ij} = \frac{q_{ij}}{M \times N} \tag{9}$$

The probability of two classes are given as:

$$\omega_0 = \sum_{i=0}^{s-1} \sum_{j=0}^{t-1} p_{ij}; \quad \omega_1 = \sum_{i=s}^{L-1} \sum_{j=t}^{L-1} p_{ij} \tag{10}$$

The intensity means of two classes and the total mean of 2D histogram are expressed as follows:

$$\begin{aligned}
\mu_0 = [\mu_{0i}, \mu_{0j}]^T &= \left[\frac{\sum_{i=0}^{s-1} \sum_{j=0}^{t-1} i p_{ij}}{\omega_0}, \frac{\sum_{i=0}^{s-1} \sum_{j=0}^{t-1} j p_{ij}}{\omega_0} \right]^T \\
\mu_1 = [\mu_{1i}, \mu_{1j}]^T &= \left[\frac{\sum_{i=s}^{L-1} \sum_{j=t}^{L-1} i p_{ij}}{\omega_1}, \frac{\sum_{i=s}^{L-1} \sum_{j=t}^{L-1} j p_{ij}}{\omega_1} \right]^T \\
\mu_T = [\mu_{Ti}, \mu_{Tj}]^T &= \left[\sum_{i=0}^{L-1} \sum_{j=0}^{L-1} i p_{ij}, \sum_{i=0}^{L-1} \sum_{j=0}^{L-1} j p_{ij} \right]^T
\end{aligned} \tag{11}$$

The between-class variance matrix $\boldsymbol{S_b}$ is defined as:

$$S_b = \sum_{k=0}^{1} \omega_k \left[(\mu_k - \mu_T) (\mu_k - \mu_T)^T \right] \tag{12}$$

By taking the trace of $\boldsymbol{S_b}$ following (8), where

$$\mu_i = \sum_{i=0}^{s} \sum_{j=0}^{t} i p_{ij}; \quad \mu_j = \sum_{i=0}^{s} \sum_{j=0}^{t} j p_{ij} \tag{13}$$

ACKNOWLEDGMENT

This work was supported by the Industrial Core Technology Development Program (10049079 , Develop of mining core technology exploiting personal big data) funded by the Ministry of Trade, Industry and Energy (MOTIE, Korea) and 2017-00655.

REFERENCES

[1] C. Deng, X. Gao, X. Li, and D. Tao, "A local tchebichef moments-based robust image watermarking," *Signal Processing*, vol. 89, no. 8, pp. 1531 – 1539, 2009.

[2] X. Gao, C. Deng, X. Li, and D. Tao, "Geometric distortion insensitive image watermarking in affine covariant regions," *IEEE Transactions on Systems, Man, and Cybernetics, Part C (Applications and Reviews)*, vol. 40, no. 3, pp. 278–286, May 2010.

[3] P.-P. Niu, X.-Y. Wang, Y.-P. Yang, and M.-Y. Lu, "A novel color image watermarking scheme in nonsampled contourlet-domain," *Expert Systems with Applications*, vol. 38, no. 3, pp. 2081 – 2098, 2011.

[4] R.-S. Run, S.-J. Horng, W.-H. Lin, T.-W. Kao, P. Fan, and M. K. Khan, "An efficient wavelet-tree-based watermarking method," *Expert Systems with Applications*, vol. 38, no. 12, pp. 14 357 – 14 366, 2011.

[5] E. Nezhadarya, Z. J. Wang, and R. K. Ward, "Robust image watermarking based on multiscale gradient direction quantization," *IEEE Trans. Inf. Forensics Security*, vol. 6, no. 4, pp. 1200–1213, Dec 2011.

[6] R. P. Singh, N. Dabas, A. Mishra, and V. Cahudhary, "On extreme learning machine for watermarking of an images in discrete wavelet transform domain," in *2014 Tenth Int. Conf. on Intelligent Information Hiding and Multimedia Signal Processing*, Aug 2014, pp. 163–166.

[7] A. Saboori and S. A. Hosseini, "A novel non-blind watermarking scheme for color image using pca transform and histogram matching technique," in *2016 10th International Symposium on Communication Systems, Networks and Digital Signal Processing (CSNDSP)*, July 2016, pp. 1–5.

[8] T. Huynh-The, O. Banos, S. Lee, Y. Yoon, and T. Le-Tien, "Improving digital image watermarking by means of optimal channel selection," *Expert Systems with Applications*, vol. 62, pp. 177 – 189, 2016.

[9] L. Jianzhuang, L. Wenqing, and T. Yupeng, "Automatic thresholding of gray-level pictures using two-dimension otsu method," in *Int. Conf. on Circuits and Systems*, Jun 1991, pp. 325–327 vol.1.

[10] J. Zhang and J. Hu, "Image segmentation based on 2d otsu method with histogram analysis," in *2008 Int. Conf. on Computer Science and Software Engineering*, vol. 6, Dec 2008, pp. 105–108.

[11] N. Otsu, "A threshold selection method from gray-level histograms," *IEEE Trans. Syst., Man, Cybern.*, vol. 9, no. 1, pp. 62–66, 1979.